

Article

Optimal Control of Electrified Powertrains in Offline and Online Application Concerning Dimensioning of Li-Ion Batteries

Felix Deufel *, Martin Gießler and Frank Gauterin 

Institute of Vehicle System Technology, Karlsruhe Institute of Technology, 76131 Karlsruhe, Germany; martin.giessler@kit.edu (M.G.); frank.gauterin@kit.edu (F.G.)

* Correspondence: felix.deufel@kit.edu

Abstract: Various energy management systems (driving strategies) have been developed to improve the efficiency of electrified vehicle drives. These include strategies from the field of offline optimization to determine the theoretical optimum for a given system, as well as online strategies designed for an on-board application in the vehicle. In this paper, investigations are performed on an SUV electrified by a 48 V hybrid system in P14 topology regarding both offline and online strategies. To calculate the global optimum, the performance of Dynamic Programming (DP) compared to an Equivalent Consumption Minimization Strategy (ECMS) with an iteratively determined equivalence factor is shown. Furthermore, with regard to online energy management strategies (EMS), it is presented how a predictive Online ECMS achieves additional fuel savings compared to a robust, non-predictive implementation. The simulation-based vehicle development allows detailed investigations regarding interactions between battery requirements and EMS. In this context, it is shown how various battery capacities are exploited by the discussed EMS.

Keywords: electrified powertrains; 48 V system; model predictive control; dynamic programming; equivalent consumption minimization strategy; real driving cycles; Li-ion battery



Citation: Deufel, F.; Gießler, M.; Gauterin, F. Optimal Control of Electrified Powertrains in Offline and Online Application Concerning Dimensioning of Li-Ion Batteries. *Vehicles* **2022**, *4*, 464–481. <https://doi.org/10.3390/vehicles4020028>

Academic Editors: Hongwen He and Mohammed Chadli

Received: 22 March 2022

Accepted: 16 May 2022

Published: 19 May 2022

Publisher's Note: MDPI stays neutral with regard to jurisdictional claims in published maps and institutional affiliations.



Copyright: © 2022 by the authors. Licensee MDPI, Basel, Switzerland. This article is an open access article distributed under the terms and conditions of the Creative Commons Attribution (CC BY) license (<https://creativecommons.org/licenses/by/4.0/>).

1. Introduction

Increasingly stringent emission limits and the overall rise in environmental awareness have led to the development of a wide range of alternative drive systems. In addition to purely electric vehicles, these also include 48 V hybrid electric vehicles (HEVs), which offer the major advantage of significantly reducing the CO₂ emissions with comparably low system expenditure, especially for inner-city driving.

The hybrid drive is characterized through component dimensioning, topology, and an energy management strategy (EMS) [1]. In the development phase for a 48 V hybrid system, besides the design of the electric motor with the associated power electronics, especially the sizing of the Li-ion battery is challenging. The aim here is to achieve the greatest reachable energy saving potential with the lowest possible battery capacity. On the one hand, this results from the fundamental economic interest in a battery that is as cost-effective as possible, since the battery is one of the main cost drivers of a 48 V system [2,3]. On the other hand, the increasing number of other electric energy consumers, including preheating of the exhaust after treatment [4], an electrical compressor [5], or chassis systems [6], means that less energy is available for the optimal EMS.

The EMS itself must ensure the optimal operation of the system functions in various driving scenarios. EMS have been the subject of intensive research for many years, with a wide variety of approaches being the subject of associated work.

In this article, a comprehensive analysis of both online and offline EMS is performed on a 48 V system using real driving cycles. Therefore, in a first step, two offline EMS are presented to find the theoretical optimum for a given system configuration. In contrast

to offline EMS, there exist online strategies for on-board use in the vehicle. Accordingly, a comparison of both a robust non-predictive and a predictive Equivalent Consumption Minimization Strategy (ECMS) is elaborated. During investigations, a special focus is placed on the interactions between the EMS and the reduction of the capacity of a 48 V Li-ion battery.

2. Related Work

EMS for HEVs have been widely investigated during the last few years. An overview of the most common methods is provided by [1,7–13]. There are different approaches to subdividing the strategies. One possible distinction is made between rule-based, optimization-based, and learning-based strategies, whereby mixed forms also exist. Furthermore, a distinction can be made between offline and online strategies: offline strategies are characterized by the requirement that the entire driving profile has to be known in advance. With the help of the respective optimizer, a specific hybrid architecture is characterized for a specific cycle—for example, regarding potentials of reduction in fuel consumption. In other words, for a given driving cycle, the global optimum is identified, which is calculated for benchmark analysis. In online optimization, however, only restricted a priori knowledge about the future within a driving cycle is necessary. This is why online strategies aim to be utilized on-board the vehicle [14].

The focus of this work is on the comparison of optimization-based concepts, both for the online and offline field. For determination of the global optimum (offline strategies), **Dynamic Programming (DP)** is considered to be unrivaled, since, apart from the errors resulting from the necessary discretisation of the state and control variable space, it always determines the global optimum. On the other hand, it requires very high computational effort. For the application of DP to HEVs, special reference should be made to [15–17] and the corresponding further development [18].

In addition to the DP, Pontryagin's minimum principle (PMP) can be utilized to determine the global optimum. Comparisons between DP and PMP can be found in particular in [19,20]. The ECMS, which was first published by Paganelli et al. [21], can in turn be derived from the PMP.

Depending on the specific implementation, the ECMS is assigned to the offline or online strategies. Due to the equivalence of the ECMS compared to the PMP, it can be used to find the global optimum for time-invariant systems. In this case, the so-called equivalence factor is determined iteratively [22,23]. Especially due to the low computational effort, this so-called **Offline ECMS** is widely used to determine the global optimum in offline application [24]. For an investigation of topologies with several traction motors, the 2D-ECMS has been developed [25].

For an online-capable implementation of the ECMS, the concept of an SOC-dependent regulation of the equivalence factor is deployed successfully [14,26–35]. Other **Online ECMS** approaches are based on driving recognition [36] or neural networks to determine the equivalence factor [37,38]. Such data-driven ECMS methods also include those considering reinforcement learning in the ECMS approach [39], as well as approaches using a fuzzy controller [40–43].

Regarding the use of predictive information, it was shown that a non-predictive Online ECMS concept for online application can be improved considering predictive information [44]. Apart from this, there also exist predictive Online ECMS approaches, where predictions are mandatory for the basic functionality of the ECMS [28,45]. Such control systems, in which the optimal control is determined taking into account the corresponding prediction horizon, are generally referred to as model predictive control (MPC). For an MPC, also several alternative optimizers other than ECMS can be applied, as presented in [46–48]. Here, for example, also approximated approaches of the DP (ADP) are used, whereby, due to the significantly reduced computational effort, an online capability of the DP can be realized [49,50]. In recent years, however, a variety of other approaches have been developed in which the strategy is based purely on Artificial Intelligence [51–53].

It should be clearly noted that there are countless other studies on EMS for HEVs. The authors would like to limit themselves here to the approaches most relevant to this work.

The analysis of the state of the art reveals that a comprehensive investigation of both online and offline EMS focusing on dimensioning of Li-ion batteries in 48 V HEVs using real driving cycles has not been undertaken yet. In particular, the proposed comparison of a robust non-predictive in contrast to an intuitive predictive Online ECMS should be emphasized here, whereby the main idea is based on the papers [35,44]. The basic procedure of the investigations proposed in this paper is shown in Figure 1. The variables will be explained in more detail in the following sections.

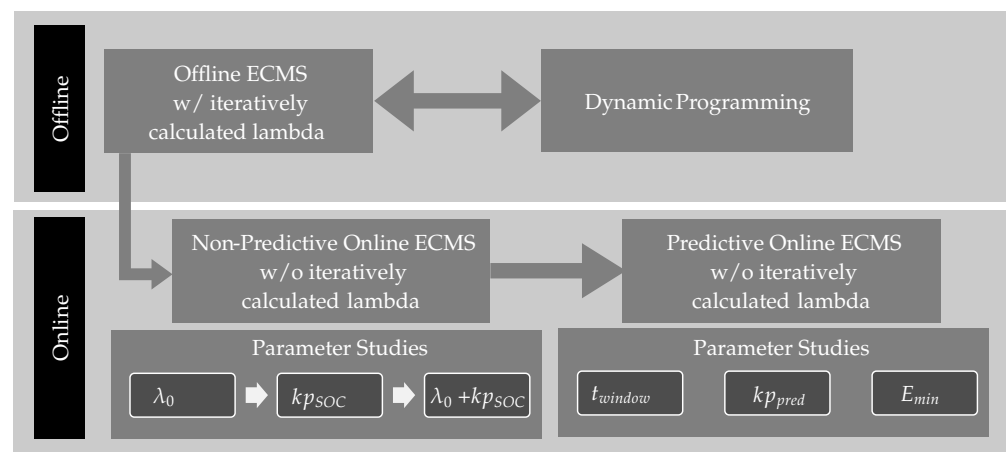


Figure 1. Applied methodology to determine optimal control in offline and online application.

3. Modeling

In the field of vehicle simulation, a distinction is made between forward and backward simulation. Forward simulation models represent the physical causality of the system: with the help of a driver model (e.g., a PID controller), the desired speed is compared with the actual vehicle speed. Based on the acceleration resulting from the control input of the driver model, a speed can then be determined in each time step. In contrast, a backward simulation model assumes that the vehicle follows a predefined speed and acceleration profile. Thus, no driver model is required. The individual advantages and disadvantages can be found in [9]. In this paper, the validated backward calculation model of a 48 V HEV including an Offline ECMS with an iteratively determined λ from the work by [24] is applied. The 48 V battery is represented by a simple inner resistance model. Hereby, Equations (1) and (2) are used both to compute the battery voltage under load U_{bat} and the corresponding battery current I_{bat} . Therefore, the battery power P_{em} , the battery losses $P_{em,loss}$, and the power from auxiliary consumers P_{aux} are considered. Moreover, the open-circuit voltage U_{OCV} and the inner resistance R_i are required. In addition, as a measure of energy deviation from the starting conditions, an energy deviation dE from reference SOC is calculated (Equation (3)). It is used as a criterion for a neutral energy balance.

$$I_{bat} = \frac{P_{em} + P_{em,loss} + P_{aux}}{U_{bat}} \tag{1}$$

$$U_{bat} = U_{OCV}(SOC) - R_i(SOC) \cdot I_{bat} \tag{2}$$

$$dE = \int U_{bat} I_{bat} dt \tag{3}$$

The battery is of a nickel–mangan–cobalt/graphite cell type, whereby R_i and U_{OCV} are calculated using SOC-specific component data. However, to ensure time-invariant properties, a constant absolute state of charge ($SOC = 70\%$) is used for the calculation of battery parameters. Other effects, such as degradation of the battery and its impact on CO_2

emissions, are neglected [24]. The model is coupled with the *dpm function* provided by ETH Zurich [15–17]. The studies are performed on an SUV hybridized in a P14 topology including two electric motors on positions P1 and P4. Figure 2 shows common topologies of HEVs in parallel configuration. The most important parameters for the analyzed HEV are summarized in Table 1.

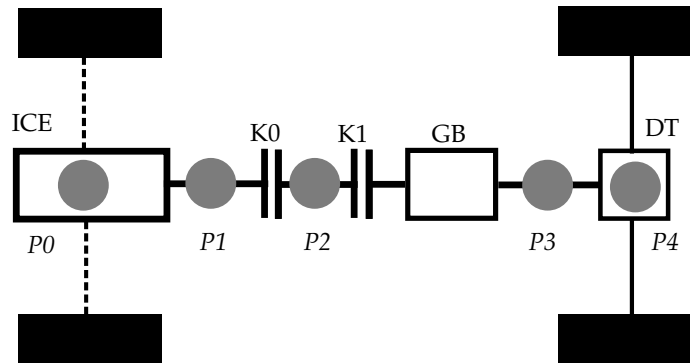


Figure 2. Topologies of HEVs in parallel configuration.

Table 1. Parameters of investigated SUV .

Frontal Area $A_f / (\text{m}^2)$	2.56
Air Drag Coefficient $c_w / (-)$	0.31
Rolling Coefficient $c_r / (-)$	0.01
Vehicle Mass $m / (\text{kg})$	1915
Wheel Radius $r_{dyn} / (\text{m})$	0.36
Power ICE $P_{ICE} / (\text{kW})$	150
Power EM $P_{EM} / (\text{kW})$	25

The investigations are based on 12 real driving cycles from [54], which represent the statistical totality of 1,000,000 km. With regard to the design of an online-capable ECMS, a particularly promising approach from [35] is being further developed. Ideas from [44] are further considered also. The goal of the investigations is to minimize fuel consumption, whereby there is a proportional relationship between fuel consumption and CO₂ emissions. The CO₂ values representing fuel consumption in this work are calculated with the relation 1 l/100 km = 23.2 g CO₂/km. The main features of the two approaches considered in this work, DP and ECMS, are described below.

3.1. Dynamic Programming (DP)

DP is based on Bellman’s principle of optimality, which states that the optimal trajectory for a discrete decision problem is also optimal for the corresponding subproblem [55]. Based on this principle, the DP is a numerical method with which the global optimal solution is found by operating backwards in time. For the application of DP, the state of charge x as well as the torque distribution u must be discretized, leading to $u_k \in U_k$ and $x_k \in \Omega_k$; see Figure 3 (left). When considering $u = \{u_0, u_1, \dots, u_{N-1}\}$ as the torque split strategy and defining the initial state as $x(0) = x_0$, then the cost function J is defined as follows [9,16].

$$J(x_0) = g_N(x_N) + \sum_{k=0}^{N-1} g_k(x_k, u_k) \tag{4}$$

$g_N(x_N)$ stands for the final costs. These are zero, in the case that $SOC(N) = SOC(0)$, to guarantee charge-sustaining (CS) operation, and infinite otherwise. The cost function g_k is the fuel consumption of the combustion engine. The optimal solution J^* is written as:

$$J^*(x_0) = \min_u J(x_0, u) \tag{5}$$

As in offline optimization, the entire driving cycle is known in advance, the algorithm can proceed backward, to find the sequence of controls which generates the optimal control starting from the final step N. For more detailed information, the reader is referred to [9].

3.2. Equivalent Consumption Minimization Strategy (ECMS)

For an ECMS, as well as with the DP algorithm, the control input u has to be discretized. A discretization of x , however, is not needed. The optimal solution is found by calculating the equivalent fuel consumption considering the lower heating value of the fuel Q_{lHV} and an equivalence factor λ , which transforms the battery power into fuel power at each time step. Using the resulting fuel equivalent, a cost function J is defined, which is minimized at each time step to obtain the optimal torque split. The corresponding optimization problem P is written as [24]:

$$P : \min_u \int J(u, x) dt \tag{6}$$

$$J(u, x) = \dot{m}_{fuel} + \lambda \frac{P_{bat}}{Q_{lHV}} \tag{7}$$

The determination of λ depends on the individual implementation of the ECMS. For determination of the global optimum, λ has to be chosen constant for a time-invariant system according to the PMP. This constant λ is usually determined iteratively, as visualized in Figure 3 (right).

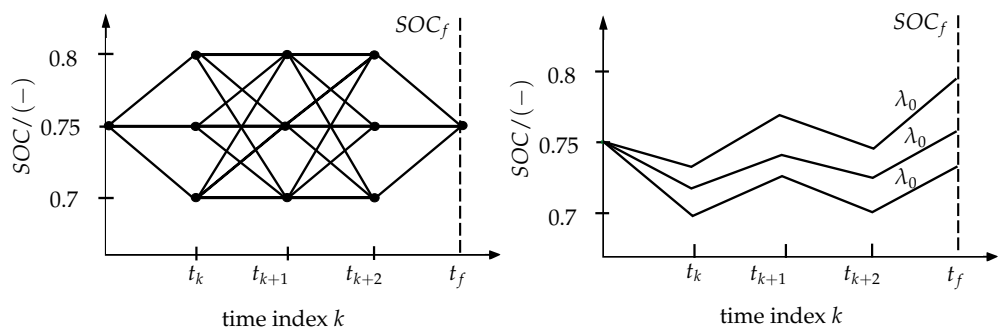


Figure 3. Principle DP (left) and ECMS with iteratively determined λ_0 (right) regarding SOC, based on [9,56]. For DP, the entire state space must be discretized to calculate the costs of any control and state combination. When applying an ECMS, no state space discretization is needed. The iteratively determined λ_0 finally leads to an optimal control ensuring CS operation.

4. Results

4.1. Global Optimum-Dynamic Programming vs. Offline ECMS

Unlimited Battery Capacity

Since the system has time-invariant properties, a constant equivalence factor λ_0 is sufficient according to PMP to determine the theoretical optimum (Equation (8)).

$$\lambda = \lambda_0 \tag{8}$$

λ_0 is iteratively calculated using the shooting method to ensure CS operation of the vehicle. Hereby, in a first step, an initial value is determined, which is based on engineering experience. After the simulation run, the actual final SOC value is compared with the desired final SOC value. Depending on whether the SOC of the battery is too high or too low, λ_0 is adjusted accordingly and the cycle is run again, until a suitable λ_0 is found [9,56]. Table 2 lists the minimum CO₂ emissions for the 12 real driving cycles for both the DP and the Offline ECMS including λ_0 . λ_0 enables the Offline ECMS to calculate the optimum trajectory for the respective cycle, while at the same time ensuring CS operation.

The presented CO₂ emissions result for the respective fuel-optimal trajectory. The deviations are <1%, which is why the results are considered equivalent at this point. The remain-

ing deviations result from numerical errors and the fundamentally different functionality of the two EMS; see Section 3.

Table 2. Comparison of CO₂ emissions in Offline ECMS vs. DP (unlimited battery capacity).

Road Type	Driving Style	CO ₂ DP g/km	CO ₂ OfflineECMS g/km	λ ₀ (ECMS Only)
urban low	aggressive	147.9	147.5	2.92
urban low	average	136.2	136.7	3.00
urban low	mild	123.9	124.3	3.14
urban high	aggressive	120.6	121.6	3.14
urban high	average	107.4	108.2	3.17
urban high	mild	106.4	106.5	3.19
extra-urban	aggressive	169.7	169.7	3.06
extra-urban	average	136.4	135.6	2.97
extra-urban	mild	131.1	131.3	2.99
highway	aggressive	246.4	245.2	3.20
highway	average	220.5	221.4	3.18
highway	mild	204.3	205.7	3.21

Limited Battery Capacity

As mentioned in the Introduction, this work pays special attention to the interactions between the selected EMS and the sizing of the battery. Therefore, in Figure 4, Offline ECMS and DP are compared regarding the calculation of the global optimum for different battery capacities. As can be seen, the Offline ECMS cannot ensure optimal operation of the HEV when reducing the energy content of the battery. As a result of the reduced energy content of the battery, time-variant effects occur due to the frequent reaching of the respective SOC limits. With a battery capacity of 100 Wh, the calculated trajectory of the ECMS can deviate by 30% from the optimum; for 25 Wh, the deviation rises up to 45%. It can be concluded that the optimum battery size should be determined with the DP approach, since an Offline ECMS with iteratively determined λ is less accurate.

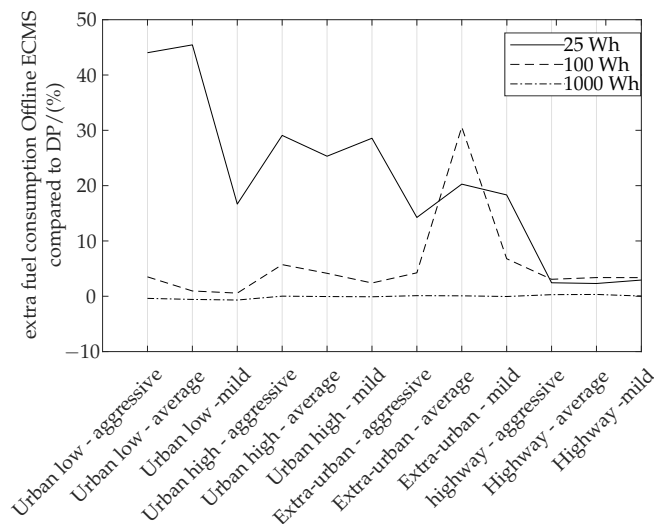


Figure 4. Comparing Offline ECMS and DP to calculate the global optimum (fuel consumption) for different battery capacities: extra fuel consumption of an Offline ECMS when limiting battery capacity to 25 Wh, 100 Wh, and 1000 Wh.

When applying DP, as in in Figure 5, the fundamental usefulness of considering batteries with low energy content is proven. It becomes clear that partly similar savings effects (extra fuel consumption < 2%) are achieved for a 25 Wh battery compared to the large battery—for example, for *highway aggressive* and *urban low mild* cycles.

As presented in Figure 5, it should also be mentioned that there is a small increase in fuel consumption at 1000 Wh compared to the 100 Wh variant (negative values). This results from the coarser discretization due to the constant amount of interpolation points in combination with the increased battery capacity; see principles of the DP demonstrated in Figure 3.

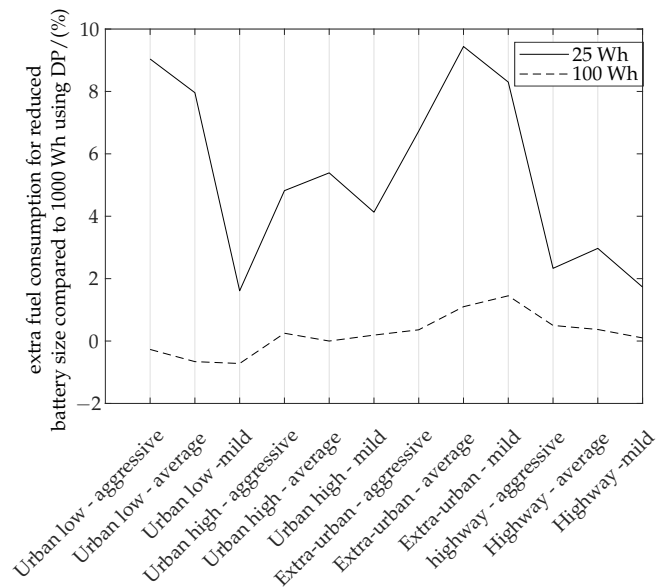


Figure 5. Using DP to analyze the global optimum (fuel consumption) for different battery capacities: extra fuel consumption when reducing the battery capacity to 25 Wh and 100 Wh compared to 1000 Wh.

To sum up, for powertrain design, DP is preferable to Offline ECMS, especially in terms of battery sizing. It is shown that even smaller batteries of 25 Wh or 100 Wh show savings potentials similar to those of a 1000 Wh battery for certain driving cycles and should therefore be considered in powertrain design. Since the previous studies focused on purely offline investigations, the following will examine how the different battery sizes behave in an on-board implementation.

4.2. Online ECMS (Non-Predictive)

In the following, the parameterization of a robust, non-predictive Online ECMS is presented. This also includes discussions of the chosen battery size and the parametrization of the robust non-predictive Online ECMS.

Unlimited Battery Capacity

As shown in Table 2, the suitable equivalence factors for the 12 real driving cycles considered range between $\lambda_0 = 2.92$ and $\lambda_0 = 3.21$. Based on the determined equivalence factors for the different driving cycles, an average equivalence factor is determined, which can serve as an initial value for a non-predictive Online ECMS. Assuming that real-world operation is represented by equal weighting of all cycles, the arithmetic mean of all cycles is determined for a first calculation of a non-predictive Online ECMS ($\lambda_{0,avg} = 3.01$). Without further measures, this does not ensure CS behavior in online operation. The SOC trajectories lead to excessive charging or discharging of the battery depending on the cycle (see principles of the ECMS demonstrated in Figure 3). The simplest measure here is the introduction of an additional penalty term in the calculation of λ (Equation (8)). Hereby, the value of the energy ($=\lambda$) is either increased or decreased depending on the deviation $dSOC$ of the actual SOC from the reference SOC. According to [35,56], the penalty via a trigonometric function is preferable to a proportional one: it permits small deviations from the reference SOC but large deviations are severely penalized. Therefore, the penalty term consists of the penalty factor kp_{SOC} multiplied by the cubic derivation of SOC $dSOC^3$ (Equation (9)).

$$\lambda = \lambda_0 - kp_{SOC} \cdot dSOC^3 \quad (9)$$

As already mentioned, it is assumed that real-world operation is represented by an equal weighting of all given cycles. Furthermore, expert discussions define the requirement for the EMS that the final deviation of the energy content of the battery at the end of cycle is restricted to ± 100 Wh regarding CS operation. Based on these assumptions, an appropriate kp_{SOC} for the non-predictive Online ECMS is determined. Table 3 reveals that kp_{SOC} has to be raised to up to 191.92, to keep the energy deviation dE_{end} from the reference SOC within the allowed range of ± 100 Wh for the *extra-urban average* cycle ($\lambda_0 = 3.01$). The extra consumption is up to 2.90% higher compared to the global optimum determined from the DP.

Table 3. Results of the non-predictive Online ECMS for $\lambda_0 = 3.01$, $kp_{SOC} = 191.92$, and $|dE_{end}| < 100$ Wh for an unlimited battery.

Road Type	Driving Style	dE_{end} Wh	$CO_{2Online} ECMS$ g/km	Extra Fuel Consumption Global Optimum (DP Solution) %
urban low	aggressive	53.48	150.82	1.96
urban low	average	37.63	138.05	1.38
urban low	mild	-7.52	124.14	0.27
urban high	aggressive	36.96	122.32	1.33
urban high	average	-27.65	108.62	1.07
urban high	mild	2.47	107.89	1.34
extra-urban	aggressive	58.33	172.23	1.36
extra-urban	average	99.34	139.63	2.32
extra-urban	mild	73.53	135.00	2.90
highway	aggressive	68.14	250.74	1.76
highway	average	65.94	222.88	1.02
highway	mild	43.5	206.10	0.85

With the aid of these preliminary investigations using an unlimited battery capacity, basic knowledge regarding a suitable choice of λ_0 and kp_{SOC} was gained. In the following, an optimal battery-specific parametrization of λ_0 and kp_{SOC} should be found. This also takes into account factor interactions of both parameters.

Limited Battery Capacity

Figure 6 reveals the CO_2 emissions for a 25 Wh battery for different parametrizations of the Online ECMS over the selected λ_0 and the selected kp_{SOC} . It is shown that the CO_2 emissions over all cycles depend almost exclusively on the selected λ_0 , which is noticeable by the strip-like structure. The influence of kp_{SOC} , on the other hand, is almost negligible.

In contrast to the results of a 25 Wh battery (Figure 6), for the 100 Wh battery, a high dependence of fuel consumption on both kp_{SOC} and λ_0 can be observed (Figure 7). It can be seen that a higher kp_{SOC} reduces the influence of λ_0 on the achievable low fuel consumption (dark blue region). On the other hand, kp_{SOC} should not be chosen to be too high, since this restricts hybrid operation. Nevertheless, for both analyzed battery capacities, the lowest CO_2 emissions are achieved with an equivalence factor of $\lambda_0 \approx 3$.

Moreover, as seen in Figure 8, for the 1000 Wh battery, the lowest consumptions are also found around $\lambda_0 \approx 3$. Parametrizations in which CS cannot be observed are clearly indicated by corresponding white areas. For these parameterizations, kp_{SOC} is chosen to be too low, so the boundary condition of ± 100 Wh final SOC cannot be guaranteed. Consequently, λ_0 must be selected perfectly for each cycle in order to guarantee CS operation.

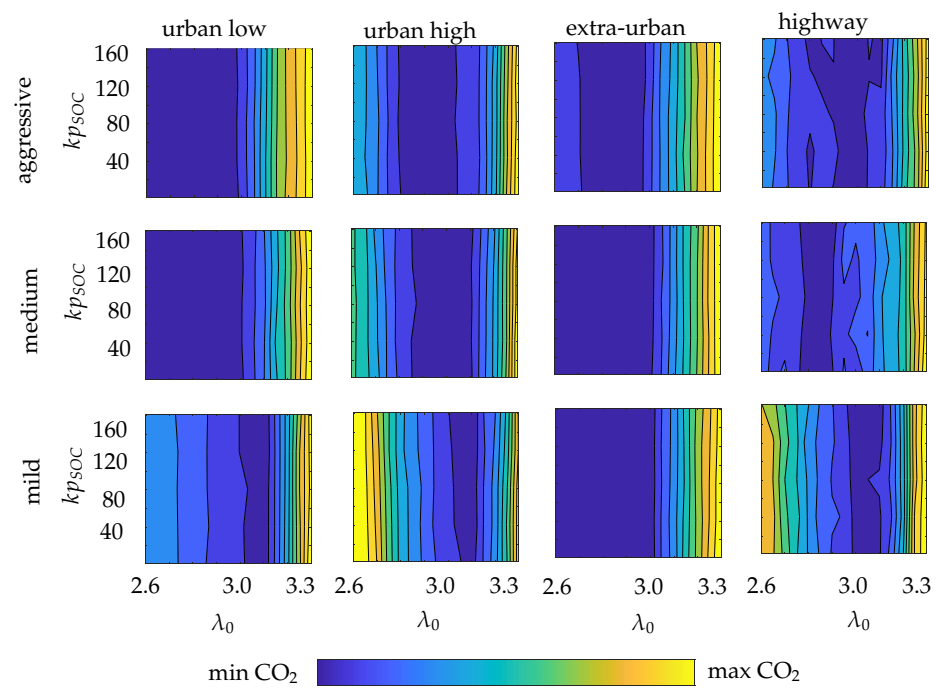


Figure 6. Parameter studies for both k_{pSOC} and λ_0 for Online ECMS (25 Wh battery).

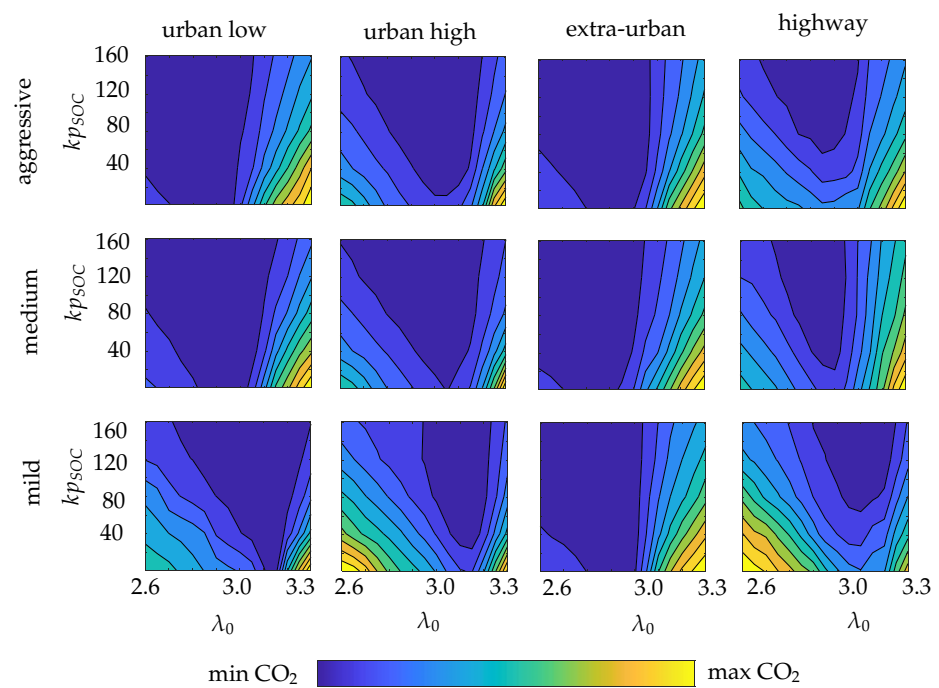


Figure 7. Parameter studies for both k_{pSOC} and λ_0 for Online ECMS (100 Wh battery).

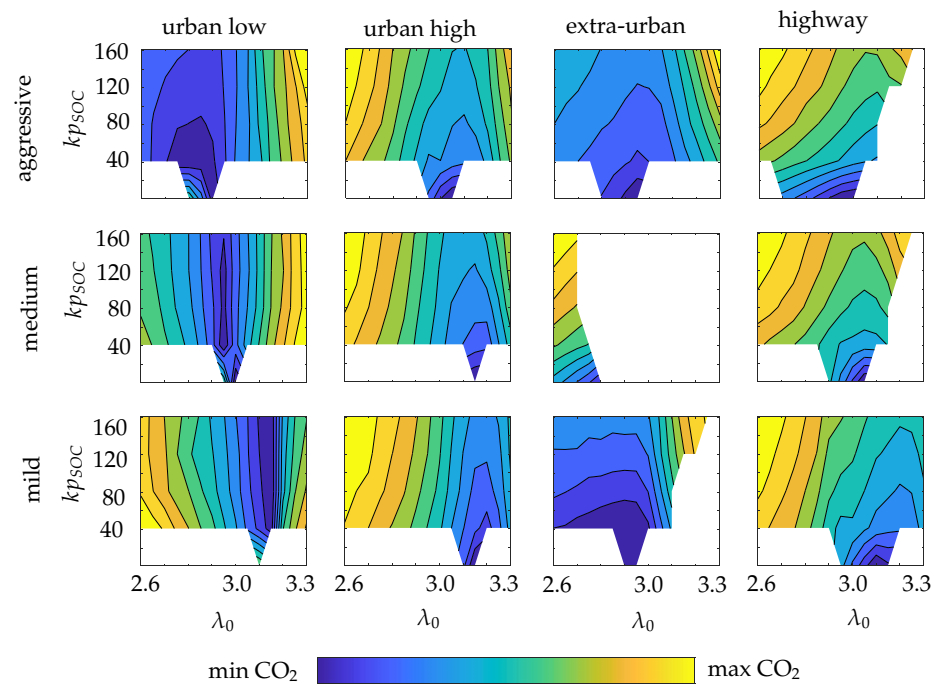


Figure 8. Parameter studies for both kp_{SOC} and λ_0 for Online ECMS (1000 Wh battery).

Next, the battery-specific ideal parametrization of the Online ECMS is selected. This parametrization is characterized by the smallest mean deviation from the global optimum over all 12 cycles. Final parameters are listed in Table 4. Along the lines of the Offline ECMS in Section 4.1, the increase in fuel consumption compared to the global optimum (DP solution) decreases with a larger battery (3.41%→0.88%).

Table 4. Final parameters appropriate selection of kp_{SOC} and λ_0 for the Online ECMS.

Battery Size Wh	λ_0	kp_{SOC}	∅ Extra Fuel Consumption Global Optimum (DP Solution) %
25	2.90	161	3.41
100	2.90	121	1.23
1000	2.85	41	0.88

The cycle-specific results are presented in Figure 9. For the variant with 1000 Wh and 100 Wh battery, the deviation of the non-predictive Online ECMS from the DP solution is max. 2%. For the 25 Wh battery, the fuel consumption is raised and shows a clear downward trend over the cycles. An analysis of the SOC trajectories clearly indicates that for cycle *urban low-mild* (+6.6%), the selected λ_0 tends to be lower compared to the iteratively determined one ($\lambda_{0,Online} = 2.90$ vs. $\lambda_{0,Offline} = 3.14$). As a result, the SOC is permanently at the lower SOC limit, which in turn significantly restricts the hybrid functionalities. For the *extra-urban aggressive* cycle, on the other hand, the lambda value from the online implementation is closer to that from the Offline ECMS ($\lambda_{0,Online} = 2.90$ vs. $\lambda_{0,Offline} = 3.06$; see Table 2). The small difference of $\lambda_0 = 3.06$ and $\lambda_0 = 3.14$ underlines the high sensitivity of the ECMS with regard to the selected λ_0 .

Deviations $\lambda_{0,Online}$ to $\lambda_{0,Offline}$ in the *highway* cycles are even significantly greater with up to $\lambda_{0,Offline} = 3.21$. However, since the 48 V system can only achieve a very limited reduction in consumption on the motorway due to the high power levels [24], even a not ideally set Online ECMS only leads merely to a slight increase in fuel consumption.

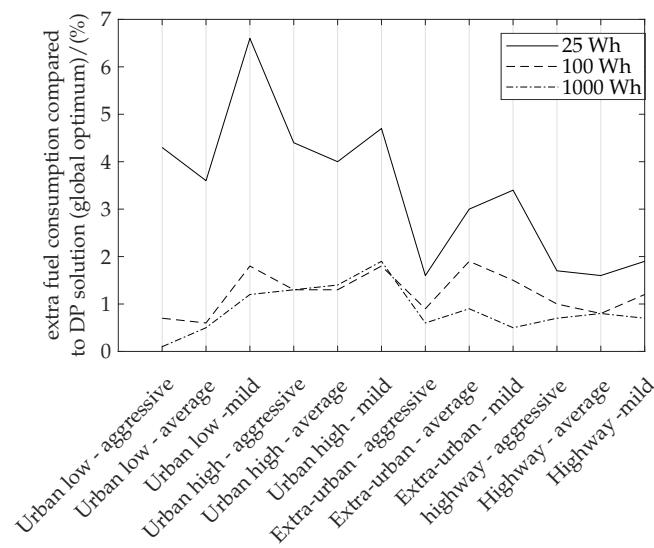


Figure 9. Extra fuel consumption of proposed non-predictive Online ECMS compared to the global optimum (DP solution) regarding fuel consumption.

To sum up, with regard to online implementation on-board, a non-predictive implementation of an Online ECMS already approaches the global optimum when choosing a large battery within powertrain design. However, if smaller batteries in the order of 25 Wh or 100 Wh are considered, the fuel consumptions deviate significantly from the global optimum. Thus, a high potential for improvement by incorporating predictive information is expected. Therefore, it is demonstrated in the following, by the example of a 25 Wh battery, how an additional reduction in consumption is possible by taking into account predictive information.

4.3. Online ECMS (Predictive)

In the context of this work, the objective is to fulfill the premise of a predictive Online ECMS that is understood intuitively. While the optimizer from energy management basically determines the best possible operation from a number of potential operating modes [56], there are a few operating modes that are not further determined by the optimizer and are therefore not part of the optimization problem. One of these is the recuperation mode. As long as the component limits are not exceeded and there is residual capacity in the battery, recuperation is carried out when possible. The exact amount of energy that is recuperated can vary depending on the specific application. Further influences on recuperation are neglected within the presented studies. This also includes the influence of dynamic wheel load changes.

The developed approach of a predictive Online ECMS is based on the following idea: using a simple longitudinal dynamics model, the resulting recuperation potential at the wheel is determined from the predicted torque demand within the prediction horizon. Neglecting the efficiency of the drivetrain, this results in a measure of the guaranteed SOC increase within the prediction horizon. According to this predicted energy increase, the value of the electrical energy (=the value of the equivalence factor λ) is preventively lowered by the introduction of an additional term $kp_{pred} \cdot p_{recu}$ (Equation (10)). p_{recu} represents the recuperation potential in the prediction horizon in Wh; kp_{pred} is a proportionality factor to be parameterized.

$$\lambda = \lambda_0 - kp_{SOC} \cdot dSOC^3 - kp_{pred} \cdot p_{recu} \quad (10)$$

As described, a lower λ means a reduction in the value of the electrical energy in the ECMS. In consequence, the battery is rather discharged in advance. Especially in the case of small batteries, the benefit of recuperation potential from the driving cycle is raised by

less reaching the SOC limits in recuperation phases. Hereby, consequently, additional fuel saving potentials can be achieved.

In the case of large batteries, the predictive Online ECMS has a similar effect. However, for large batteries, individual recuperation phases rarely lead to reaching the limits. To achieve savings potential, a reduction in the penalty of the SOC deviation kp_{SOC} can be realized without violating the defined boundary conditions for a robust CS operation ($|dE_{end}| < 100$ Wh). A reduction in the penalty of the SOC deviation kp_{SOC} in turn results in more degrees of freedom in the EMCS. Since the effects of a reduction in battery capacity are the focus in this work, merely an additional term is added to the existing parametrization. Further adjustments of the robust non-predictive implementation from the section above are not carried out.

In the following, the influence of the prediction horizon is presented. Moreover, an additional parameter is introduced, which specifies the minimum amount of energy from which the recuperated energy is considered.

Prediction Horizon $t_{horizon}$

Figure 10 shows the influences of a small (10 s) and a large (50 s) prediction horizon illustrated on two sequences from a real driving cycle. In both cases, the SOC curve and speed were plotted. Additionally, in the case on the left, the wheel torque was plotted. In the case on the right, the torque of the combustion engine is shown.

As presented in *Sequence 1*, a consideration of the recuperation potential with a time horizon of 10 s at $t = 770$ s is limited. The battery is not discharged properly; in consequence, SOC_{Max} is already reached at an early point in time of the recuperation phase (red line). In order to take into account a higher amount of recuperation potential from deceleration, a larger prediction horizon of 50 s should be considered (blue dotted line in SOC). On the other hand, regarding *Sequence 2*, a prediction horizon of 50 s can also lead to recuperation potentials being taken into account too early in the predictive Online ECMS. At $t = 280$ s, for example, due to an insufficient state of charge resulting from the future recuperation potential, the ICE is activated. In consequence, this leads to an increase in fuel consumption.

The wheel torque is not shown in *Sequence 2*. The decrease in speed at $t = 290$ s can be seen on the lines of a negative wheel torque. It can be concluded that the selected prediction horizon majorly influences the EMS.

Threshold E_{min}

In the following, the introduction of a threshold is discussed. Therefore, in Figure 11, λ and SOC are plotted over time. On the left, only λ is plotted for both a predictive Online ECMS and a non-predictive Online ECMS *without* a threshold. On the right, the same plot is presented *with* a threshold. Additionally, for the case *with* the threshold, the SOC is introduced on the right.

The consideration of the recuperation potential by introducing the term $kp_{pred} \cdot p_{recu}$ (Equation (10)) leads to a continuous reduction in λ compared to the non-predictive Online ECMS without further measures in Figure 11 (left). This is problematic, as explained in the following: according to [49,56], in the case of time-invariant properties of the battery, a constant λ leads to a global optimal control, when it is determined as described in Section 3.2. The proposed non-predictive Online ECMS includes an average value for λ_0 over the 12 real driving cycles. The resulting λ is further adjusted via kp_{SOC} in the non-predictive implementation to ensure CS operation in the Online ECMS. Although global optimal operation cannot be reached using this non-predictive Online ECMS, the best possible alignment to the λ_0 values that lead to an optimal solution for the individual cycles is achieved. In the case of a continuous reduction, λ deviates significantly from the iteratively determined values. Due to the resulting always lower λ (=low value of the electrical energy), the battery is always discharged sooner, which leads to an overall significantly lower SOC trajectory. This results in an increase in fuel consumption due to the restricted hybrid functionality. To avoid such continuous reduction in λ , a threshold is introduced. A minimum amount of recuperable energy E_{min} is necessary for an intervention in the lambda calculation (see Figure 11, middle plot). An intervention to λ should be only

allowed if as much recuperation potential is expected that the additional deviation from the averaged λ_0 value is overcompensated by the fuel savings potential resulting from $k_{pred} \cdot p_{recu}$. Overall, the resulting SOC trajectories remain quite similar; see Figure 11, right. However, the influence of the predictive Online ECMS is clearly visible in the SOC plot at $t = 1600$ s (see Figure 11, zoom view right plot).

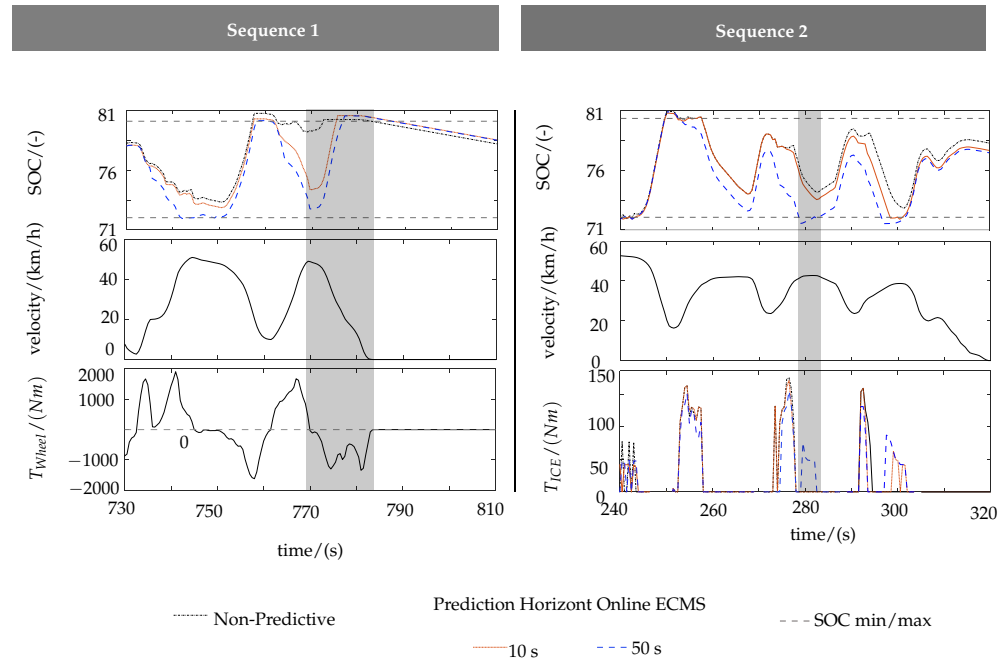


Figure 10. Analysis regarding the prediction horizon of the proposed predictive Online ECMS in two exemplary sequences.

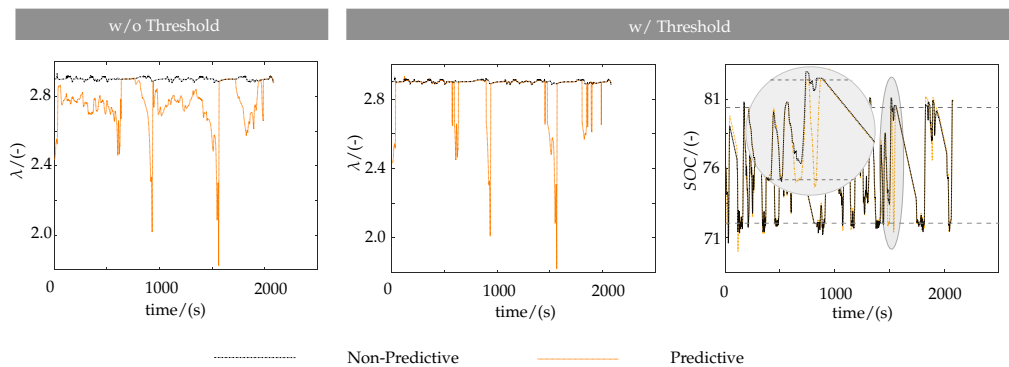


Figure 11. Analysis regarding introduction of a threshold to the proposed predictive Online ECMS, without and with threshold. Non-predictive Online ECMS (black) and predictive Online ECMS (orange). Considering recuperation potential as introduced in Equation (10) results in a continuous reduction in λ without any further measures (see without threshold) for the predictive Online ECMS (orange).

Finally, in the context of the procedure for the non-predictive Online ECMS, parameter studies are performed. The boundaries of the three parameters to be examined are listed in Table 5.

Table 5. Range of parameter studies of the predictive Online ECMS.

$k_{pred}(-)$	$t_{horizon}(s)$	$E_{min}(Wh)$
0.001...0.029	10...100	5...100

From these parameter studies, the ideal parameterization for the predictive Online ECMS is specified. Results show a significant reduction potential compared to the non-predictive Online ECMS; see Table 6. A robust parametrization results in up to 1.65% saving potentials in the *urban-low aggressive* cycle. In individual cycles, a slight increase in fuel consumption is observed for the robust parametrization. An average saving potential of 0.4% can be expected when all saving potentials are equally weighted. In the case of cycle-specific parametrization, the saving potentials rise up to 2.32% compared to the purely non-predictive Online ECMS. On average, a savings potential of 0.7% can be expected here. An individual parametrization of the ECMS must not be completely ruled out, but further algorithms are necessary in order to be able to adapt the parametrization of the predictive Online ECMS to on-board use.

A closer look at the columns on the right in Table 6 (→ individual parametrization) indicates that $\lambda_0 = 2.90$ of the Online ECMS for cycles *urban low mild*, *urban high average*, *urban high mild* tends to be lower compared to the iteratively determined values (Table 2). Since the battery SOC hardly reaches the upper SOC limit, the predictive Online ECMS in the form described offers only very limited saving potentials, since only a reduction in λ is possible. In other cycles, significantly greater savings effects are observed, as the non-predictive Online ECMS often reaches SOC_{Max} . The analyses reveal that cycles must be checked individually to understand the resulting fuel saving potentials and take appropriate measures. It must be considered when recuperation potentials occur while the SOC trajectory is at SOC_{min} and how to handle this. Many recuperation potentials can only be taken into account to a limited extent. In other cycles, the non-existent savings potentials simply result from relatively low recuperation potentials in the cycle overall. Moreover, in the context of the non-predictive variant, in the case of high power requirements, there is a limited influence of the hybrid functionality through the 48 V system overall (e.g., on *highway* cycles). In this case, a predictive control will not lead to any measurable additional fuel savings.

Consequently, in a follow-up work, a dependency of kp_{pred} on SOC is introduced. Thus, if the battery state of charge at time t_k is already at SOC_{min} , no additional reduction in the value of the electrical energy (λ) is allowed. Furthermore, a dependence of kp_{pred} on the occurrence of the recuperation potential in the predicted horizon can be implemented. If the recuperation occurs early in the time horizon, a large influence is aimed at; if it occurs late in the horizon, a small influence should be realized. Moreover, the predictive Online ECMS algorithm is to be further developed by taking stationary phases or pure e-drive phases into account. Here, the demand for the ICE is smaller than the minimum threshold for activation of the ICE, which is why it is expected that the auxiliary consumers or traction are supplied purely from the electrical energy storage.

In this section, additional findings are proposed with regard to an implementation on-board. It is proven that in the case of choosing a small battery in powertrain design, a predictive Online ECMS can achieve significant reduction potentials in fuel consumption compared to a robust, non-predictive implementation. The suggested predictive Online ECMS, which takes into consideration the future recuperation potential, offers savings potentials of up to 2.32% when compared to the robust, non-predictive Online ECMS with a 25 Wh battery.

Table 6. Results of proposed Online ECMS with robust (left) as well as individual parametrization (right) for a 25 Wh battery using $\lambda_0 = 2.90$ and $kp_{SOC} = 161$.

		Robust Parametrization				Individual Parametrization			
		kp_{pred}	$t_{horizons}$	E_{min} Wh	%*	kp_{pred}	$t_{horizons}$	E_{min} Wh	%*
Urban low	aggressive	0.015	10	20	1.65	0.015	20	20	2.32
Urban low	average	0.015	10	20	1.80	0.009	20	10	1.82
Urban low	mild	0.015	10	20	−0.47	0.005	100	20	0.18
Urban high	aggressive	0.015	10	20	0.54	0.015	10	20	0.54
Urban high	average	0.015	10	20	−0.30	0.007	100	10	0.00
Urban high	mild	0.015	10	20	−0.05	0.003	10	5	0.02
Extra-urban	aggressive	0.015	10	20	0.14	0.029	10	20	0.24
Extra-urban	average	0.015	10	20	0.38	0.025	10	5	0.90
Extra-urban	mild	0.015	10	20	0.78	0.029	10	5	1.39
Highway	aggressive	0.015	10	20	0.26	0.021	10	10	0.32
Highway	average	0.015	10	20	0.18	0.019	10	5	0.31
Highway	mild	0.015	10	20	0.06	0.019	20	5	0.18

* Reduction in fuel consumption compared to proposed robust Online ECMS.

5. Conclusions

A research study into both online and offline energy management strategies (EMS) concentrating on the dimensioning of Li-ion batteries in 48 V HEVs by using real driving cycles is presented in this publication. This includes, in particular, a comparison of a robust non-predictive Online ECMS to an intuitive predictive Online ECMS. Therefore, investigations were performed on an SUV electrified by a 48 V hybrid system in P14 topology.

It is demonstrated how two widespread approaches from the field of offline strategies perform for determining the global optimum as a function of battery size (capacity). It can be seen that with the 100 Wh battery, there is up to +30% deviation from the global optimum when applying an Offline ECMS compared to DP. For the battery of 25 Wh, the deviation increases up to +50%. Thus, DP is identified as a suitable optimizer for the proposed investigations. Using DP, it is presented that even a smaller battery of 25 or 100 Wh shows similar savings potentials in certain cycles as when using the 1000 Wh battery. This motivates deeper investigations regarding reduced battery capacity.

Furthermore, in the field of online strategies, it is worked out how a predictive Online ECMS can achieve additional savings compared to a purely robust, non-predictive implementation. Therefore, it is demonstrated in a first step that the proposed non-predictive Online ECMS leads merely to an additional consumption of $\approx 1\%$, compared to the global optimum in the case of a 1000 Wh battery. With a 25 Wh battery, the additional consumption increases to $\approx 5\%$. It is concluded that with a large battery, the non-predictive variant of an Online ECMS already closely approaches the global optimum. In other words, the potential for improvement through predictive implementation is very limited for the 1000 Wh battery. For a 25 Wh battery, however, it is revealed that the proposed predictive Online ECMS, in which the future recuperation potential is taken into account, shows savings potentials of up to 2.32% compared to the robust, non-predictive Online ECMS variant.

The predictive Online ECMS algorithm will be improved in the future by taking into consideration stand phases or pure e-drive phases. It is also possible to make kp_{pred} SOC-dependent or dependent on the exact appearance of the recuperation potential in the predicted horizon.

Author Contributions: Conceptualization, F.D.; methodology, F.D.; software, F.D.; validation, F.D.; formal analysis, F.D.; investigation, F.D.; resources, F.D.; data curation, F.D.; writing—original draft preparation, F.D.; writing—review and editing, F.D.; visualization, F.D.; supervision, M.G. and F.G. All authors have read and agreed to the published version of the manuscript.

Funding: This research was funded by Mercedes-Benz AG.

Institutional Review Board Statement: Not applicable.

Informed Consent Statement: Not applicable.

Data Availability Statement: Not applicable.

Acknowledgments: The authors would like to thank Mercedes-Benz AG for funding this project. We acknowledge support by the KIT-Publication Fund of the Karlsruhe Institute of Technology.

Conflicts of Interest: The authors declare no conflict of interest.

References

1. Silvas, E.; Hofman, T.; Murgovski, N.; Etman, P.; Steinbuch, M. Review of Optimization Strategies for System-Level Design in Hybrid Electric Vehicles. *IEEE Trans. Veh. Technol.* **2017**, *66*, 57–70. [[CrossRef](#)]
2. Vora, A.P.; Jin, X.; Hoshing, V.; Shaver, G.; Varigonda, S.; Tyner, W.E. Integrating battery degradation in a cost of ownership framework for hybrid electric vehicle design optimization. *Proc. Inst. Mech. Eng. Part D J. Automob. Eng.* **2019**, *233*, 1507–1523. [[CrossRef](#)]
3. Cardoso, D.S.; Fael, P.O.; Espírito-Santo, A. A review of micro and mild hybrid systems. *Energy Rep.* **2020**, *6*, 385–390. [[CrossRef](#)]
4. Liu, Y.; Canova, M.; Wang, Y.Y. Distributed Energy and Thermal Management of a 48-V Diesel Mild Hybrid Electric Vehicle with Electrically Heated Catalyst. *IEEE Trans. Control Syst. Technol.* **2020**, *28*, 1878–1891. [[CrossRef](#)]
5. Griefnow, P.; Andert, J.; Xia, F.; Klein, S.; Stoffel, P.; Engels, M.; Jolovic, D. *Real-Time Modeling of a 48V P0 Mild Hybrid Vehicle with Electric Compressor for Model Predictive Control*; SAE International: Warrendale, PA, USA, 2019. [[CrossRef](#)]
6. Tschöke, H.; Gutzmer, P.; Pfund, T. (Eds.) *Elektrifizierung des Antriebsstrangs*; Springer: Berlin/Heidelberg, Germany, 2019. [[CrossRef](#)]
7. Tran, D.D.; Vafaeipour, M.; El Baghdadi, M.; Barrero, R.; van Mierlo, J.; Hegazy, O. Thorough state-of-the-art analysis of electric and hybrid vehicle powertrains: Topologies and integrated energy management strategies. *Renew. Sustain. Energy Rev.* **2020**, *119*, 109596. [[CrossRef](#)]
8. Serrao, L. A Comparative Analysis of Energy Management Strategies for Hybrid Electric Vehicles. Ph.D. Thesis, The Ohio State University, Columbus, OH, USA 2009.
9. Onori, S.; Serrao, L.; Rizzoni, G. *Hybrid Electric Vehicles*; Springer: London, UK, 2016. [[CrossRef](#)]
10. Rizzoni, G.; Onori, S. Energy Management of Hybrid Electric Vehicles: 15 years of development at the Ohio State University. *Oil Gas Sci. Technol. Rev. D'IFP Energies Nouv.* **2015**, *70*, 41–54. [[CrossRef](#)]
11. Salmasi, F.R. Control Strategies for Hybrid Electric Vehicles: Evolution, Classification, Comparison, and Future Trends. *IEEE Trans. Veh. Technol.* **2007**, *56*, 2393–2404. [[CrossRef](#)]
12. Xu, N.; Kong, Y.; Chu, L.; Ju, H.; Yang, Z.; Xu, Z.; Xu, Z. Towards a Smarter Energy Management System for Hybrid Vehicles: A Comprehensive Review of Control Strategies. *Appl. Sci.* **2019**, *9*, 2026. [[CrossRef](#)]
13. Jiang, Q.; Ossart, F.; Marchand, C. Comparative Study of Real-Time HEV Energy Management Strategies. *IEEE Trans. Veh. Technol.* **2017**, *66*, 10875–10888. [[CrossRef](#)]
14. Chasse, A.; Sciarretta, A.; Chauvin, J. Online optimal control of a parallel hybrid with costate adaptation rule. *IFAC Proc. Vol.* **2010**, *43*, 99–104. [[CrossRef](#)]
15. Sundström, O. Optimal Hybridization in Two Parallel Hybrid Electric Vehicles using Dynamic Programming. *IFAC Proc. Vol.* **2008**, *41*, 4642–4647. [[CrossRef](#)]
16. Sundstrom, O.; Guzzella, L. A generic dynamic programming Matlab function. In Proceedings of the 2009 IEEE Control Applications, (CCA) & Intelligent Control, (ISIC), St. Petersburg, Russia, 8–10 July 2009; pp. 1625–1630. [[CrossRef](#)]
17. Sundström, O.; Ambühl, D.; Guzzella, L. On Implementation of Dynamic Programming for Optimal Control Problems with Final State Constraints. *Oil Gas Sci. Technol. Rev. De L'Institut Français Du Pétrole* **2010**, *65*, 91–102. [[CrossRef](#)]
18. Elbert, P.; Ebbesen, S.; Guzzella, L. Implementation of Dynamic Programming for n -Dimensional Optimal Control Problems with Final State Constraints. *IEEE Trans. Control Syst. Technol.* **2013**, *21*, 924–931. [[CrossRef](#)]
19. Kim, N.; Cha, S.; Peng, H. Optimal Control of Hybrid Electric Vehicles Based on Pontryagin's Minimum Principle. *IEEE Trans. Control Syst. Technol.* **2011**, *19*, 1279–1287. [[CrossRef](#)]
20. Kim, N.; Rousseau, A. Sufficient conditions of optimal control based on Pontryagin's minimum principle for use in hybrid electric vehicles. *Proc. Inst. Mech. Eng. Part D J. Automob. Eng.* **2012**, *226*, 1160–1170. [[CrossRef](#)]
21. Paganelli, G.; Delprat, S.; Guerra, T.M.; Rimaux, J.; Santin, J.J. Equivalent consumption minimization strategy for parallel hybrid powertrains. In Proceedings of the IEEE 55th Vehicular Technology Conference, VTC Spring 2002 (Cat. No. 02CH37367), Birmingham, AL, USA, 6–9 May 2002; pp. 2076–2081. [[CrossRef](#)]
22. Serrao, L.; Onori, S.; Rizzoni, G. ECMS as a realization of Pontryagin's minimum principle for HEV control. In Proceedings of the 2009 American Control Conference, St. Louis, MO, USA, 10–12 June 2009; pp. 3964–3969. [[CrossRef](#)]
23. Zheng, C.H. Numerical Comparison Of Ecms And Pmp-Based Optimal Control Strategy In Hybrid Vehicles. *Int. J. Automot. Technol.* **2014**, *15*, 1189–1196. [[CrossRef](#)]
24. Foerster, D.; Decker, L.; Doppelbauer, M.; Gauterin, F. Analysis of CO₂ reduction potentials and component load collectives of 48 V-hybrids under real-driving conditions. *Automot. Engine Technol.* **2021**, *6*, 45–62. [[CrossRef](#)]

25. Mayer, A. Two-Dimensional ECMS for System Analysis of Hybrid Concepts featuring Two Electric Traction Motors. In Proceedings of the 2019 International Symposium on Systems Engineering (ISSE), Edinburgh, UK, 1–3 October 2019.
26. Onori, S.; Serrao, L. On Adaptive-ECMS strategies for hybrid electric vehicles. In Proceedings of the Les Rencontres Scientifiques d'IFP Energies Nouvelles–International Conference on Hybrid and Electric Vehicles–RHEVE 2011, Rueil-Malmaison, France, 6–7 December 2011.
27. Onori, S.; Serrao, L.; Rizzoni, G. Adaptive Equivalent Consumption Minimization Strategy for Hybrid Electric Vehicles. In Proceedings of the ASME 2010 Dynamic Systems and Control Conference DSCC2010, Cambridge, MA, USA, 12–15 September 2010.
28. Musardo, C.; Rizzoni, G.; Staccia, B. *A-ECMS: An Adaptive Algorithm for Hybrid Electric Vehicle Energy Management: Proceedings, Seville, Spain, 12–15 December 2005*; IEEE Operations Center: Piscataway, NJ, USA, 2005.
29. Kessels, J.; Koot, M.; van den Bosch, P.; Kok, D.B. Online Energy Management for Hybrid Electric Vehicles. *IEEE Trans. Veh. Technol.* **2008**, *57*, 3428–3440. [[CrossRef](#)]
30. Liu, T.; Zou, Y.; Liu, D.X.; Sun, F.C. Real-time control for a parallel hybrid electric vehicle based on Pontryagin's Minimum Principle. In Proceedings of the 2014 IEEE Conference and Expo Transportation Electrification Asia-Pacific (ITEC Asia-Pacific), Beijing, China, 31 August–3 September 2014; pp. 1–5. [[CrossRef](#)]
31. Ouddah, O.; Aduane, L.; Abdrakhmanov, R. From Offline to Adaptive Online Energy Management Strategy of Hybrid Vehicle Using Pontryagin's Minimum Principle. *Int. J. Automot. Technol.* **2017**, *19*, 571–584. [[CrossRef](#)]
32. Sivertsson, M. Adaptive Control Using Map-Based ECMS for a PHEV. *IFAC Proc. Vol.* **2012**, *45*, 357–362. [[CrossRef](#)]
33. Zhang, F.; Xu, K.; Li, L.; Langari, R. Comparative Study of Equivalent Factor Adjustment Algorithm for Equivalent Consumption Minimization Strategy for HEVs. In Proceedings of the 2018 IEEE Vehicle Power and Propulsion Conference (VPPC), Chicago, IL, USA, 27–30 August 2018; pp. 1–7. [[CrossRef](#)]
34. Fu, Z.; Liu, X. Equivalent Consumption Minimization Strategy Based on a Variable Equivalent Factor. In Proceedings of the IEEE 2017 Chinese Automation Congress (CAC), Jinan, China, 20–22 October 2017. [[CrossRef](#)]
35. Enang, W.; Bannister, C. Robust proportional ECMS control of a parallel hybrid electric vehicle. *Proc. Inst. Mech. Eng. Part D J. Automob. Eng.* **2017**, *231*, 99–119. [[CrossRef](#)]
36. Gu, B.; Rizzoni, G. An Adaptive Algorithm for Hybrid Electric Vehicle Energy Management Based on Driving Pattern Recognition. In Proceedings of the ASME International Mechanical Engineering Congress and Exposition, Chicago, IL, USA, 5–10 November 2006.
37. Chen, Z.; Liu, Y.; Zhang, Y.; Lei, Z.; Chen, Z.; Li, G. A neural network-based ECMS for optimized energy management of plug-in hybrid electric vehicles. *Energy* **2021**, *243*, 122727. [[CrossRef](#)]
38. Xie, S.; Hu, X.; Qi, S.; Lang, K. An artificial neural network-enhanced energy management strategy for plug-in hybrid electric vehicles. *Energy* **2018**, *163*, 837–848. [[CrossRef](#)]
39. Lee, H.; Cha, S.W. Reinforcement Learning Based on Equivalent Consumption Minimization Strategy for Optimal Control of Hybrid Electric Vehicles. *IEEE Access* **2021**, *9*, 860–871. [[CrossRef](#)]
40. Zhang, F.; Xi, J.; Langari, R. An adaptive equivalent consumption minimization strategy for parallel hybrid electric vehicle based on Fuzzy PI. In Proceedings of the 2016 IEEE Intelligent Vehicles Symposium (IV), Gothenburg, Sweden, 19–22 June 2016; pp. 460–465. [[CrossRef](#)]
41. Li, L.; Huang, H.; Lian, J.; Yao, B.; Zhou, Y.; Chang, J.; Zheng, N. Research of Ant Colony Optimized Adaptive Control Strategy for Hybrid Electric Vehicle. *Math. Probl. Eng.* **2014**, *2014*, 1–10. [[CrossRef](#)]
42. Wang, S.; Huang, X.; Lopez, J.M.; Xu, X.; Dong, P. Fuzzy Adaptive-Equivalent Consumption Minimization Strategy for a Parallel Hybrid Electric Vehicle. *IEEE Access* **2019**, *7*, 133290–133303. [[CrossRef](#)]
43. Zhang, F.; Liu, H.; Hu, Y.; Xi, J. A Supervisory Control Algorithm of Hybrid Electric Vehicle Based on Adaptive Equivalent Consumption Minimization Strategy with Fuzzy PI. *Energies* **2016**, *9*, 919. [[CrossRef](#)]
44. Kural, E.; Güvenc, B.A. Predictive-Equivalent Consumption Minimization Strategy for Energy Management of A Parallel Hybrid Vehicle for Optimal Recuperation. *J. Polytech.* **2015**, *2015*, 113–124.
45. Gao, A.; Deng, X.; Zhang, M.; Fu, Z. Design and Validation of Real-Time Optimal Control with ECMS to Minimize Energy Consumption for Parallel Hybrid Electric Vehicles. *Math. Probl. Eng.* **2017**, *2017*, 1–13. [[CrossRef](#)]
46. Huang, Y.; Wang, H.; Khajepour, A.; He, H.; Ji, J. Model predictive control power management strategies for HEVs: A review. *J. Power Sources* **2017**, *341*, 91–106. [[CrossRef](#)]
47. Josevski, M.; Abel, D. Energy Management of Parallel Hybrid Electric Vehicles based on Stochastic Model Predictive Control. *IFAC Proc. Vol.* **2014**, *47*, 2132–2137. [[CrossRef](#)]
48. Zhou, Q.; Du, C. A quantitative analysis of model predictive control as energy management strategy for hybrid electric vehicles: A review. *Energy Rep.* **2021**, *7*, 6733–6755. [[CrossRef](#)]
49. Wahl, H.G. Optimale Regelung eines Prädiktiven Energiemanagements von Hybridfahrzeugen. Ph.D. Thesis, Institute of Vehicle System Technology, Karlsruhe Institute of Technology, Karlsruhe, Germany, 2015.
50. Bauer, K.L. Echtzeit-Strategieplanung für Vorausschauendes Automatisiertes Fahren. Ph.D. Thesis, Institute of Vehicle System Technology, Karlsruhe Institute of Technology, Karlsruhe, Germany, 2020.
51. Lian, R.; Tan, H.; Peng, J.; Li, Q.; Wu, Y. Cross-Type Transfer for Deep Reinforcement Learning Based Hybrid Electric Vehicle Energy Management. *IEEE Trans. Veh. Technol.* **2020**, *69*, 8367–8380. [[CrossRef](#)]

52. Liu, T.; Tang, X.; Wang, H.; Yu, H.; Hu, X. Adaptive Hierarchical Energy Management Design for a Plug-In Hybrid Electric Vehicle. *IEEE Trans. Veh. Technol.* **2019**, *68*, 11513–11522. [[CrossRef](#)]
53. Maino, C.; Mastropietro, A.; Sorrentino, L.; Busto, E.; Misul, D.; Spessa, E. Project and Development of a Reinforcement Learning Based Control Algorithm for Hybrid Electric Vehicles. *Appl. Sci.* **2022**, *12*, 812. [[CrossRef](#)]
54. Forster, D.; Inderka, R.B.; Gauterin, F. Data-Driven Identification of Characteristic Real-Driving Cycles Based on k-Means Clustering and Mixed-Integer Optimization. *IEEE Trans. Veh. Technol.* **2020**, *69*, 2398–2410. [[CrossRef](#)]
55. Bellman, R. *Dynamic Programming*, 1st ed.; Princeton University Press: Princeton, NJ, USA, 1957.
56. Görke, D. *Untersuchungen zur Kraftstoffoptimalen Betriebsweise von Parallelhybridfahrzeugen und Darauf Basierende Auslegung Regelbasierter Betriebsstrategien*; Springer: Wiesbaden, Germany, 2016. [[CrossRef](#)]